Electronic Supplementary Material (ESI) for Green Chemistry.

Tailoring Diesel Bioblendstock from Integrated Catalytic Upgrading of Carboxylic Acids: A "Fuel Property First" Approach

Xiangchen Huo[a,b], Nabila A. Huq[a], Jim Stunkel[a], Nicholas S. Cleveland[a], Anne K. Starace[a], Amy E. Settle[a,b], Allyson M. York[a,b], Robert S. Nelson[a], David G. Brandner[a], Lisa Fouts[a], Peter C. St. John[a], Earl D. Christensen[a], Jon Luecke[a], J. Hunter Mack[c], Charles S. McEnally[d], Patrick A. Cherry[d], Lisa D. Pfefferle[d], Timothy J. Strathmann[b], Davinia Salvachúa[a], Seonah Kim[a], Robert L. McCormick[a], Gregg T. Beckham[a], Derek R. Vardon[a]*

[a]National Renewable Energy Laboratory, 15013 Denver West Parkway, Golden, CO, United States
[b]Colorado School of Mines, 1500 Illinois St., Golden, CO, United States
[c]University of Massachusetts Lowell, 220 Pawtucket St., Lowell, MA, United States
[d]Yale University, 9 Hillhouse Avenue, New Haven, CT, United States
*Derek.Vardon@nrel.gov

Section S1: Experimental Methods

Catalyst synthesis and characterization

Pt/Al_2O_3 catalyst was prepared by strong electrostatic adsorption method with chloroplatinic acid hexahydrate as Pt precursor. Al_2O_3 of 30-50 mesh and Pt precursor were added to deionized water, and solution pH was adjusted to 3 by adding HCl. After stirring overnight, the catalyst particles were recovered by filtration extensively washed with deionized water. The catalyst was dried in the air and reduced in flowing H_2 (200 mL min^{-1}) at 300°C for 4 h.

BET surface area was determined by nitrogen physisorption using a Quadrasorb SI™ surface area analyzer from Quantachrome Instruments. Samples of ~80–120 mg were measured using a 55-point nitrogen adsorption/desorption curve at -196°C. Prior to analysis, the samples were degassed at 300°C for 16 h under vacuum. BET surface areas were calculated over a relative pressure range of 0.050 to 0.250 P/P_0. The surface area measurements are within 10% of deviation.

Pt dispersion on alumina was measured from CO pulse chemisorption performed using an Altamira AMI-390 micro-flow reactor system equipped with a thermal conductivity detector (TCD). Samples of ~50–100 mg were loaded in a quartz U-tube reactor and heated in 5% H_2/Ar to 250°C at 5 °C min^{-1} with a hold time of 2 h. After the reduction step, catalyst samples were flushed with He at 50 mL min^{-1} for 1 h, cooled to 30 °C and dosed with sequential 500-μL pulses of 10% CO/He mixture. A 500-μL sample loop was used to calibrate the TCD response for CO after each experiment. Pt dispersion was calculated by assuming a Pt:CO stoichiometry of one-to-one.

The total number of acid sites was determined by NH_3 pulse chemisorption using the same Altamira Instruments AMI-390 system. Samples of ~100–150 mg were loaded in a quartz U-tube reactor. ZrO_2 samples were pretreated under flowing He at 5 °C min^{-1} to 350°C and then held at this temperature for 2 h. Nb_2O_5 samples were pretreated under flowing He at 5°C min^{-1} to 300°C with a hold time of 2 h. Pt/Al_2O_3 samples were pretreated under flowing 5% H_2/Ar to 300°C at 5°C min^{-1} with a hold time of 2 h. The samples were cooled to 120°C under flowing He and dosed with sequential 2000-μL pulses of 10% NH_3/He mixture. A 2000-μL sample loop was used to calibrate the TCD response for NH_3 after each experiment.

The relative ratio of Brønsted to Lewis acid sites was determined by pyridine adsorption diffuse reflectance Fourier transform infrared spectroscopy (py-DRIFTS). Spectra represent the average of 64 scans collected at 4 cm^{-1} resolution using a Thermo Nicolet iS50 FT-IR spectrometer equipped with a Harrick Praying Mantis reaction chamber. Oxide samples were pretreated under flowing Ar at 5°C min^{-1} to 350°C and then held at this temperature for 2 h. Pt/Al_2O_3 samples were pretreated under flowing 5% H_2/Ar to 300°C at 5°C min^{-1} with a hold time of 2 h. After cooling to 150°C at 5°C min^{-1}, the samples were purged with Ar for 10 min, and a background spectrum was collected. The samples were then exposed to pyridine vapor for 5 min by flowing Ar through a pyridine-filled bubbler held at room temperature. Physisorbed pyridine was subsequently desorbed in Ar by heating to 200°C at 5°C min^{-1} and holding for 30 min. After cooling to 150°C at 5°C min^{-1}, a spectrum was collected and referenced to the background collected prior to pyridine exposure. The peak area of vibrational modes near 1445 cm^{-1} (Lewis) and 1540 cm^{-1} (Brønsted) were used to determine the relative ratio of Brønsted to Lewis acidic sites.

The irreversibly adsorbed carbon amount of spent catalysts was measured by a Setaram Setsys Evolution thermal gravimetric analyzer (TGA) coupled with a Nicolet 6700 Fourier Transform InfraRed (FTIR) spectrometer via a transfer line heated at 200°C. The FTIR spectrometer is equipped with a gas cell maintained at 225°C to prevent vapor condensation. The catalyst was heated to 800°C under zero air (19-21% oxygen with a balance of nitrogen). The onset of carbon combustion was determined by the observation of carbon dioxide in the FTIR. Prior to the onset of carbon combustion, only water was observed in the FTIR spectra. Therefore, the carbon content was calculated by subtracting the mass loss due to water from the total mass loss recorded by the TGA.

Catalytic testing

Acid ketonization experiments were carried out in packed-bed reactor at 435°C and atmospheric pressure. The liquid flow and Ar flow rates were 0.2 mL min^{-1} and 100 mL (STP) min^{-1}, respectively. The feed was introduced to the reactor by a HPLC pump. Both the liquid feed and Ar flew downward through a ZrO_2 catalyst (Johnson Matthey, 30-50 mesh) bed in between inert 1-mm glass beads, which were held in place with quartz wool in a 0.5” OD (0.035” wall thickness) tubular stainless-steel reactor coated with a silica Dursan coating (SilcoTek Coating Co.). The reactor was heated by a tubular split furnace. A back-pressure regulator was used to control the reactor pressure (the regulator was fully open for ketonization experiments). Liquid products were collected in a knock-out pot and analyzed off-line. The gaseous products were monitored by an on-line gas chromatograph and a nondispersive infrared detector. Conversion and carbon yield are defined by the following equations:

$$\text{Conversion } = \frac{f_{Butyric\ acid,feed} - f_{Butyric\ acid,ave}}{f_{Butyric\ acid,feed}} \times 100\% \tag{1}$$

$$\text{Carbon yield} = \frac{f_{Product,ave}}{f_{Butyric\ acid,feed}} \times 100\% \tag{2}$$

where $f_{Butyric\ acid,feed}$ = molar flow rate of carbon in butyric acid in the feed; $f_{Butyric\ acid,ave}$ = average molar flow rate of carbon in butyric acid during sampling interval; $f_{Product\ ave}$ = average molar flow rate of carbon in product during sampling interval.

Ketone condensation experiments were performed in a Parr multi-batch reactor system (Parr Instrument Company). Fresh Nb_2O_5 catalyst (CBMM HY-340 calcined in static air at 350°C for 12 h) or regenerated catalyst (spent catalyst calcined in static air at 350°C for 12 h) was added to 75-mL reactor cups together with feed solution, followed by purging and flushing of the system with He for three cycles. The reactors were sealed and heated to the desired temperature over a period of ~20 min. Reaction solution and catalyst were well mixed by using magnetic stir bars operating at 800 rpm. Reactors were quenched in an ice bath to terminate the reaction at predetermined time. Products were filtered through 0.2-μm PTFE membranes to separate the liquid from the catalysts. Conversion, average rate, carbon yield and selectivity are defined by the following equations:

$$\text{Conversion } = \frac{n_{4-Heptanone,initial} - n_{4-Heptanone,t}}{n_{Reactant,initial}} \times 100\% \tag{3}$$

$$\text{Carbon yield} = \frac{n_{Product,t}}{n_{4-Heptanone,initial}} \times 100\% \tag{4}$$

$$\text{Selectivity } = \frac{Carbon\ yield}{Conversion} \times 100\% \tag{5}$$

where $n_{4-Heptanone,initial}$ = mole of carbon in 4-heptanone in the feed; $n_{4-Heptanone,t}$ = mole of carbon in reactant at a given time; $n_{Product,t}$ = mole of carbon in product at a given time.

The HDO feed was prepared by removing solvent and unreacted ketone from condensation products for recycle by distillation. The distillation was performed on a spinning band distillation column (B/R Instrument Corporation) using a reflux ratio of 20:1 at 50 mmHg. Fractions 1 and 2 were collected at 90-120°C (atmospheric equivalent temperature, AET) and 120-190°C (AET), respectively. Fraction 3 included the remaining liquid that boils at higher temperatures. Fraction 3 was directly used as feed, with exception of biologically derived condensation products. Due to limited quantity, bio-derived condensation products were mixed with cyclohexane at 20 wt.%. HDO experiments were carried out at 334°C and under a H_2 pressure of 500 psi over a Pt/Al_2O_3 catalyst (30-50 mesh) in the same flow reactor where ketonization experiments were performed. The liquid flow and H_2 flow rates were 0.1 mL min^{-1} and 165 mL (STP) min^{-1}, respectively. Conversion and carbon yield are calculated in a similar way to those in acid ketonization experiments:

$$\text{Conversion } = \frac{f_{Dimer,feed} - f_{Dimer,ave}}{f_{Dimer,feed}} \times 100\% \tag{6}$$

$$\text{Carbon yield} = \frac{f_{Product,ave}}{f_{Dimer,feed}} \times 100\% \tag{7}$$

where $f_{Dimer,feed}$ = molar flow rate of carbon in condensation dimer in the feed; $f_{Dimer,ave}$ = average molar flow rate of carbon in dimer during sampling interval; $f_{Product\ ave}$ = average molar flow rate of carbon in product during sampling interval.

Chemical analysis

For GC-FID/MS, samples were analyzed using an Agilent 7890A GC operating in split mode (25:1 split ratio). The GC was outfitted with an Agilent HP-5ms column (30 m × 0.25-mm id, 0.25-μm film), and helium was used as the carrier gas at 1.4 mL min^{-1} column flow. The injector volume was set to 1 μL using an Agilent auto-sampler. The GC method consisted of a front inlet temperature of 260°C and an oven temperature program that starts at 40°C, holding for 2 min and then ramping at 18°C min^{-1} to a temperature of 280°C before cooling down. Sample was analyzed simultaneously by a Polyarc® system/FID and 5975 mass spectrometer detector (Agilent Technologies). FID was set at 300°C, H_2 flow at 30 mL min^{-1}, air flow at 350 mL min^{-1}, and makeup flow at 20 mL min^{-1}. MS transfer line temperature was set at 293°C.

High resolution mass spectra were collected using a JEOL GCmate II double-focusing mass spectrometer (JEOL, Peabody, MA) coupled with a DSC/TGA Q600 (TA Instruments, Newcastle, DE). Liquid samples were introduced to the MS via a heated transfer line and evaporated by heating in the DSC/TGA instrument to their boiling point. Calorimetric data were not collected as the aim of these experiments were to collect mass spectra of volatilized compounds only. The ionization source was operated in electron ionization (EI) mode at 70 eV. The mass spectrometer was tuned prior to experiments to a resolving power of ≥ 6,000 (full width at half maximum (FWHM)) based on m/z 69 using the spectrum of perfluorokerosene. The full spectrum of perfluorkerosene was used for mass calibration across the range of the spectrum collected from m/z 35 to 400.

Quantitative ^{13}C NMR spectra were acquired with ~400 µL sample and included a capillary tube filled with 1 mg/mL TSP-d_4 in DMSO-d_6 for referencing. Experiments were run using a Bruker AVANCE III 600 MHz spectrometer (14.7 T) equipped with a room temperature BBO (broad band optimized) 5 mm probe head. All spectra were measured at 25°C using a 90° pulse angle, inverse-gated decoupling, 2048 scans, and a delay of either 10 or 30 s. Integrations were performed on phased and baseline-corrected spectra, with solvent peaks excluded. Distortionless Enhancement by Polarization Transfer (DEPT) experiments were run with selection angle parameter of 135° which in CH and CH_3 groups as positive peaks, and CH_2 groups as negative peaks. The coupling constant, JCH, was set to 145 Hz. All data analysis was performed in Topspin 3.6pl7.

GCxGC-TOFMS was performed with LECO Pegasus® 4D GCxGC-TOFMS operating in split mode (50:1 split ratio). The GC was outfitted a Restek RTX-5 column (10 m × 0.15-mm id, 0.18-µm film) as the primary column and an Agilent DB1701 column (1 m × 0.10-mm id, 0.10-µm film) as the secondary column. Helium was used as the carrier gas at 1.0 mL min^{-1}. The injector volume was set to 1 µL using a Gerstel MPS2® autosampler, and the inlet temperature was set at 300°C. The primary oven temperature was held at 35°C for 7 min, ramped at 5°C min^{-1} to 255°C and held for 1 min. The primary oven temperature was held at 35°C for 7 min, ramped at 5°C min^{-1} to 255°C and held for 1 min. The secondary oven temperature was set 10°C offset from the primary oven, held for 4 min, ramped at 5°C min^{-1} to 275°C and held for 2 min. Modulator Temperature was set 15°C offset from the secondary oven and tracking the secondary oven program. Modulator Time was set at 6 s modulation, 1.0 s hot pulse / 2.0 s cold pulse. The MS setting consisted of MS transfer line temperature of 250°C and scan range from 29 m/z to 350 m/z at 200 spectra s^{-1}. ChromaTOF® data acquisition software was used to collect the chromatograms.

Lignocellulosic sugars fermentation and acids separation

The production of corn stover hydrolysate from deacetylation and dilute-acid pretreatment was previously described.[1] The hydrolysate was concentrated via rotavapor to reach a sugar concentration of approximately 450 g L^{-1} (see composition in Table S5) and stored at 4ºC. Prior the fermentation, the hydrolysate was diluted with fermentation media to achieve an initial sugar (glucose, xylose, arabinose, and galactose) concentration of 65 g L^{-1}. The fermentation media consisted of yeast extract (5 g L^{-1}), peptone (10 g L^{-1}), ammonium sulfate (3 g L^{-1}), KH_2PO_4 (3.26 g L^{-1}), $MgSO_4•7H_2O$ (0.3 g L^{-1}), $CaCl_2•2H_2O$ (0.02 g L^{-1}), $FeSO_4•7H_2O$ (0.03 g L^{-1}), $MnSO_4$•H2O (0.02 g L^{-1}), cysteine-HCl (0.5 g L^{-1}) and resazurin (1 mg L^{-1}). The organism utilized for sugars conversion to carboxylic acids was *Clostridium butyricum* (ATCC 19398). This strict anaerobic bacterium was stored in sealed glycerol stocks at -80ºC and revived anaerobically in sealed serum bottles containing Reinforced Clostridial media supplemented with 20 g L^{-1} glucose and 10 g L^{-1} xylose. Cultures were incubated for ~15 h in a rotatory shaker at 37ºC and 150 rpm. Cells were then directly inoculated in two 10-L New Brunswick BioFlo®/CelliGen® 310 bioreactors (Eppendorf) at an initial optical density at 600 nm (OD_{600}) of 0.1. Nitrogen was sparged overnight (0.1 vvm) to ensure anaerobic conditions but the gas was turned off at ~7 h to reduce foaming issues. Fermentations were maintained at 37ºC and 100 rpm. The pH was initially adjusted at pH 7 and further controlled at pH 6 by the addition of 4 N NaOH to neutralize the acids. Antifoam 204 (Sigma-Aldrich) was added when required. Samples (2 mL) were taken periodically in aseptic conditions from the bioreactors to track bacterial growth (OD_{600}), sugar utilization, and acids production. The analytical methods to quantify these metabolites were previously described.[1]

To recover bio-butyric acid from the fermentation broth, cells were first removed by centrifugation at 12,000 × g during 10 min. Then, the supernatants were filtered through 0.8-0.2 µM Sartopore 2 XLG cartridges (Sartorius) and further pumped through a 10 kDa hollow fiber filter (GE Model #UFP-10-C-4X2MA) maintaining a head pressure of 10psi. After filtration, the broth, pH 6.5, was loaded with 10% w/v activated carbon and stirred for 2 hours. The activated carbon was removed using a 1L 0.45µm a PES Nalgene Rapid-Flow filter. The filtrate, pH 7.5, was further processed in 900 g batches. Each batch was concentrated to 23% of its original mass by removing water using a rotary evaporator at 30mbar and 50°C. The concentrated broth was then acidified to pH <2 using 1g H_2SO_4 (Sigma-Aldrich ACS reagent, 95.0-98.0%) per 10g of concentrated broth. The acidified concentrated broth was then extracted twice, 1:1 v/v with ethyl acetate (Sigma-Aldrich ACS reagent ≥99.5%) in a separatory funnel. The organic phase was collected, and the ethyl acetate was removed on the rotary evaporator at 150mbar and 50°C. The remaining concentrated acetic and butyric acids were further purified and separated by vacuum distillation. The spinning band distillation column (BR Instruments 800 micro fractional distillation system) was operated at 100mbar. 4 fractions were collected: impurities below 112°C, acetic acid between 112-122°C, acetic and butyric acid mixture between 122-173°C, butyric acid between 173-175°C. The concentration of ethyl acetate, acetic acid, and butyric acid in each fraction was determined in parallel with ^{1}H NMR and HPLC. Mixing several distillation fractions to obtain the desired purity and ratio of acetic and butyric acid produced the final purified mixed acid product.

Section S2: Experimental Results (in order of mention in main text)

Table S1 Model predictions of melting point, boiling point, flash point, lower heating value, cetane number, and yield sooting index (normalized to carbon number in parentheses) for mapped hydrocarbons.

No.	Structure	C No.	Melting point (°C)		Boiling point (°C)			Flash point (°C)		L-heating value (MJ/kg)			CN	YSI
			M1	M2	M1	M2	M3	M4	M5	M6	M7	M8	M9	M10
Non-cyclic branched hydrocarbons														
1	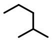	6	-131	-106	63	56	71	-29	-29	45	48	45	37	40 (6.6)
2	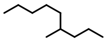	10	-86	-55	155	152	173	29	34	45	47	44	46	63 (6.3)
3	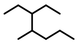	10	-101	-67	155	138	173	29	34	45	47	44	41	68 (6.8)
4	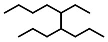	14	-56	-20	246	221	255	76	87	44	47	44	48	91 (6.5)
5	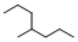	8	-109	-80	109	106	125	0	3	45	47	45	41	48 (6.0)
6	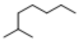	8	-109	-80	109	106	125	0	3	45	47	45	44	48 (6.0)
7	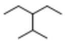	8	-124	-92	109	91	125	0	3	45	47	45	32	52 (6.5)
8	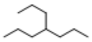	10	-86	-55	155	152	173	29	34	45	47	44	40	59 (5.9)
9	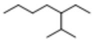	10	-101	-67	155	138	173	29	34	45	47	44	38	63 (6.3)
10	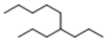	12	-64	-32	201	194	216	58	65	44	47	44	45	71 (5.9)
11	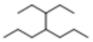	12	-79	-43	200	181	216	57	65	44	47	44	44	75 (6.2)
12	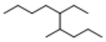	12	-79	-43	200	181	216	57	65	44	47	44	43	75 (6.2)
Cyclic hydrocarbons														
13	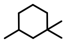	9	-55	-45	148	134	150	26	29	44	46	44	29	81 (9.0)
14	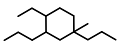	15	8	20	280	249	272	109	119	44	46	44	35	125 (8.3)
15	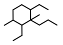	15	4	17	276	244	272	106	116	44	46	44	32	121 (8.1)
16	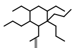	21	67	74	408	331	359	188	207	44	46	44	30	161 (7.7)
17		9	-83	-58	143	140	150	23	26	44	46	44	28	76 (8.4)
18	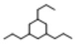	15	-16	11	280	258	272	109	120	44	46	44	39	110 (7.3)
19	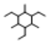	15	-29	0	266	243	272	99	110	44	46	44	29	127 (8.4)
20	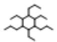	21	39	50	403	334	359	185	204	44	46	44	32	161 (7.7)
21	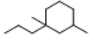	11	-33	-21	193	178	196	55	60	44	46	44	37	87 (7.9)
22	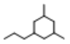	11	-61	-34	188	184	196	51	57	44	46	44	38	87 (7.9)
23	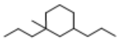	13	-10	2	239	218	236	83	92	44	46	44	37	99 (7.6)
24	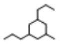	13	-38	-11	234	222	236	80	88	44	46	44	44	99 (7.6)
25	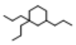	15	12	24	285	254	272	112	123	44	46	44	35	110 (7.3)
26	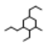	15	-20	7	275	253	272	105	116	44	46	44	38	116 (7.7)
27	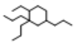	17	31	41	326	282	304	137	151	44	46	44	34	127 (7.5)
28	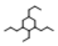	17	3	28	321	286	304	134	148	44	46	44	40	127 (7.5)
29	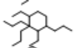	19	49	58	367	308	333	163	179	44	46	44	32	144 (7.6)
30	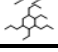	19	21	33	362	311	333	159	176	44	46	44	34	144 (7.6)

M1: ChemDraw[2]. M2: EPISuite[3]. M3: Satou (1992)[4]. M4: Prugh (1973)[5]. M5: Butler (1956)[6]. M6: Lloyd (1980)[7]. M7: Mott (1940)[8]. M8: Boie (1953)[9]. M9: Kessler (2017)[10]. M10: Das (2018)[11]. Note: Representative cyclic hydrocarbons were included from ketone cross-condensation reactions due to the large number of possible molecules.

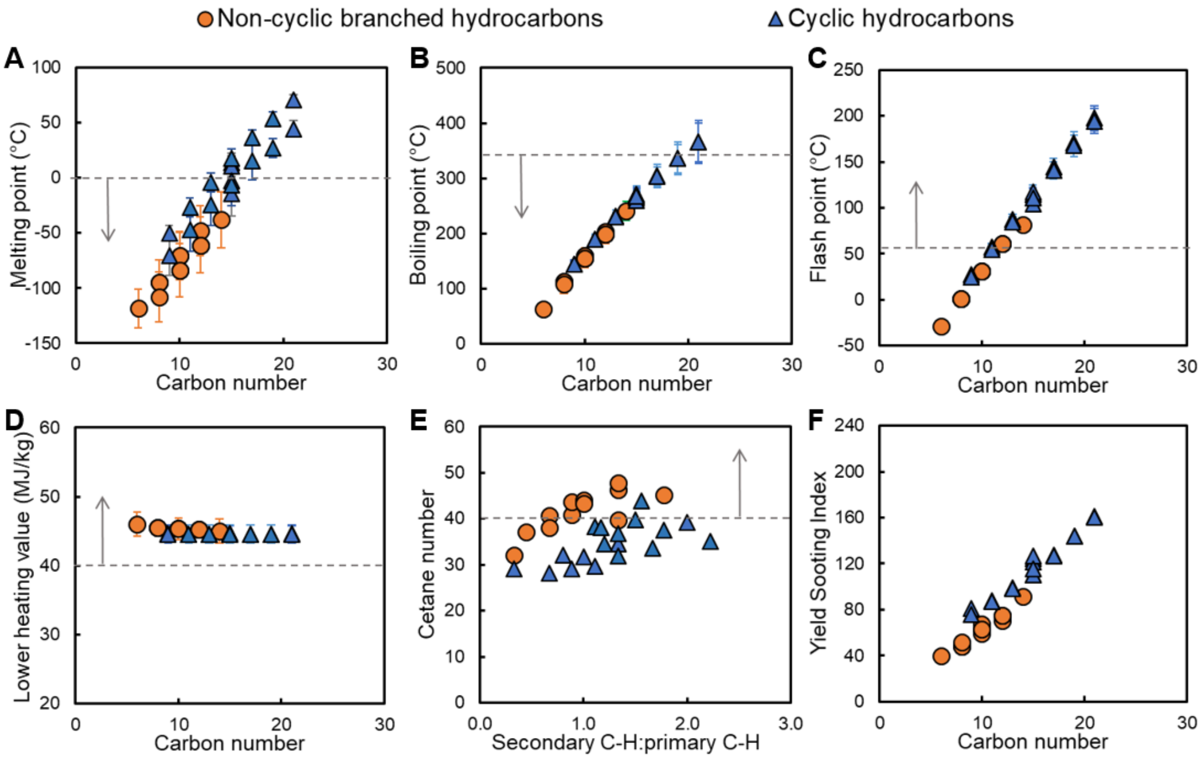

Figure S1 Plot of model predictions of (A) melting point, (B) boiling point, (C) flash point, (D) lower heating value, (E) cetane number, and (F) yield sooting index. Error bars represent standard deviations of multiple model predictions summarized in Table S1. Grey dash lines and arrows represent screening criteria.

Table S2 Surface area, acidity and metal dispersion of fresh ZrO_2, Nb_2O_5, and Pt/Al_2O_3.

Catalyst	Surface area ($m^2\ g^{-1}$)	Total acid sites (μmol g^{-1})	Brønsted acid sites (μmol g^{-1})	Lewis acid sites (μmol g^{-1})	Metal dispersion
ZrO_2	65	163	22	141	NA
Nb_2O_5	137	255	49	206	NA
Pt/Al_2O_3	198	329	27	302	9.4%

NA = Not applicable

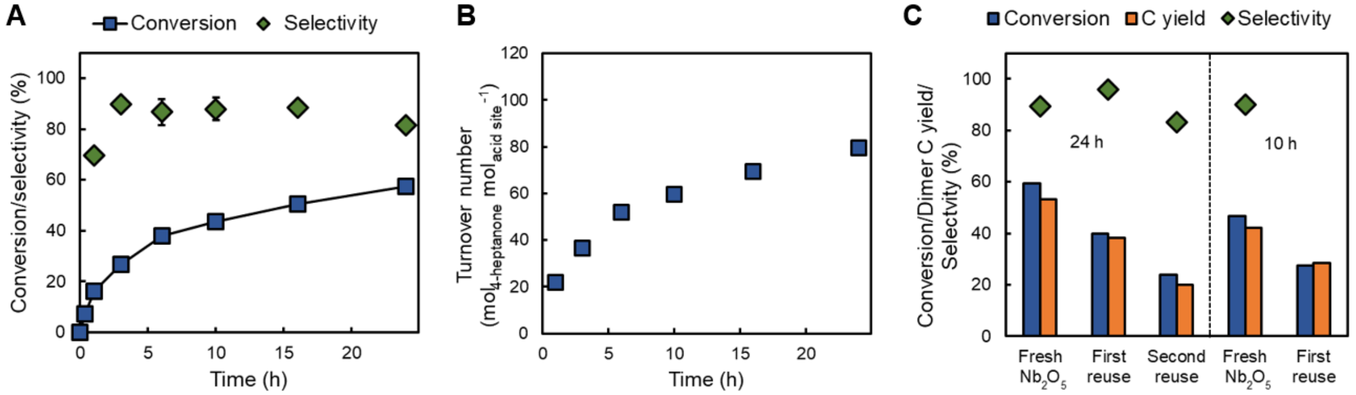

Figure S2 (A) Conversion of commercial 4-heptanone and selectivity to dimer with reaction time (15 g feed, 20 wt.% 4-heptanone in toluene, 0.75 g fresh Nb_2O_5, catalyst-to-ketone mass ratio = 1:4, 180°C). (B) Increasing turnover number for 4-heptanone condensation with reaction time (same reaction as figure A). (C) Performance of recycled catalyst (15 g feed, 20 wt.% 4-heptanone in toluene, 0.75 g spent catalyst after washing with solvent and drying at room temperature, catalyst-to-ketone mass ratio = 1:4, 180°C, 10 h or 24 h). All experiments were conducted in an initial He headspace at atmospheric pressure, stirring 800 rpm.

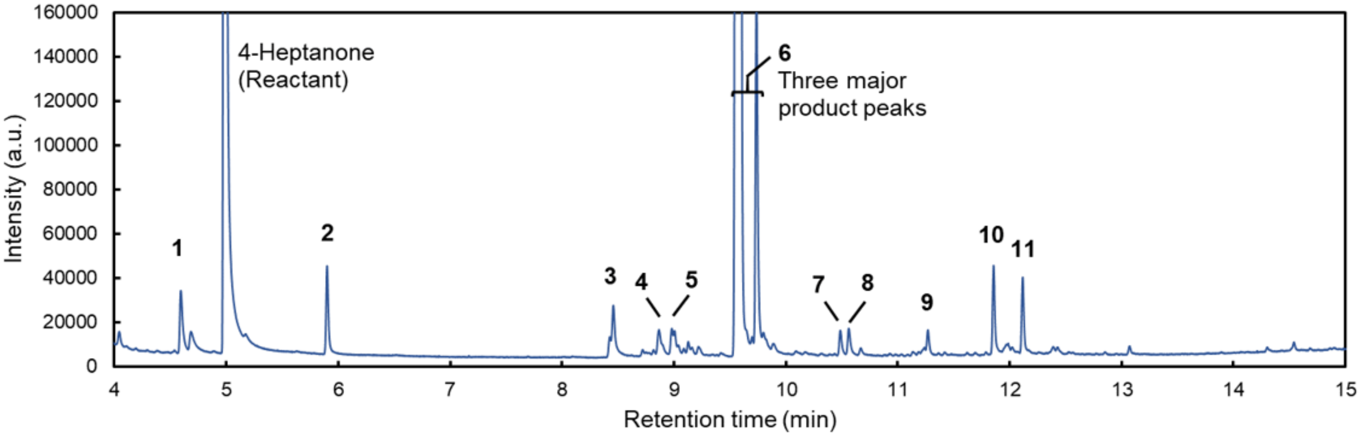

Peak #	Ret Time (min)	Compound[a]	Prob%	Potential C number	FID area relative to major product peaks
1	4.594	3-Hexanone, 2-methyl-	32.8	7	1.9%
2	5.900	3-Heptene, 4-propyl-	69.8	10	2.1%
3	8.458	3-Nonen-2-one, 3-ethyl	6.7	<14	2.5%
4	8.866	5-Ethyl-3-nonen-6-one	7.4	<14	1.2%
5	8.981	2-Pentanone, 1-(2,4,6-trihydroxyphenyl)	46.8	14	1.5%
6	9.52-9.95	Three major product peaks		14	
7	10.487	2-Allyl-5-ethoxy-4-methoxyphenol	10.6	≤14	0.7%
8	10.561	2,4,4-Trimethyl-3-(3-methylbutyl)cyclohex-2-enone	10.6	≤14	0.8%
9	11.269	10α-Eremophila-7,11-dien-9-one, 8,12-epoxy-	11.5	>14	0.6%
10	11.856	2H-Benzopyran-2-one, 4-methyl-3-phenyl-	10.7	>14	2.1%
11	12.116	Benzene, 1,2,4,5-tetrakis(1-methylethyl)-	54.7	>14	1.9%

[a] Compound of highest probability identified in NIST database

Figure S3 A typical GC-Polyarc/FID chromatogram of organic phase product from 4-heptanone condensation using GC-FID/MS method described in S1 Experimental Methods, Chemical analysis. Three major product peaks between 9.52-9.95 min exhibited significant peak intensity, so the scale was adjusted to highlight minor components. Note that heavier condensation oligomers may not show on the chromatogram. The high intensity of major product peaks allowed the identification of parent ion mass 210, consistent with condensation dimer formula ($C_{14}H_{26}O$). Details on mass spectra of the major product peaks are presented in **Figure S4**. Condensation byproducts showed up as low intensity peaks on the chromatogram, making it challenging to confirm the parent ion mass or to identify molecular structure. A list of compounds with the highest matching probability based on NIST database is provided. While the presence of dimer isomers in minor components cannot be ruled out, carbon yield and selectivity calculations for condensation dimer only considered the three major product peaks, considering minor compounds showed a low FID peak area relative to the major product peaks.

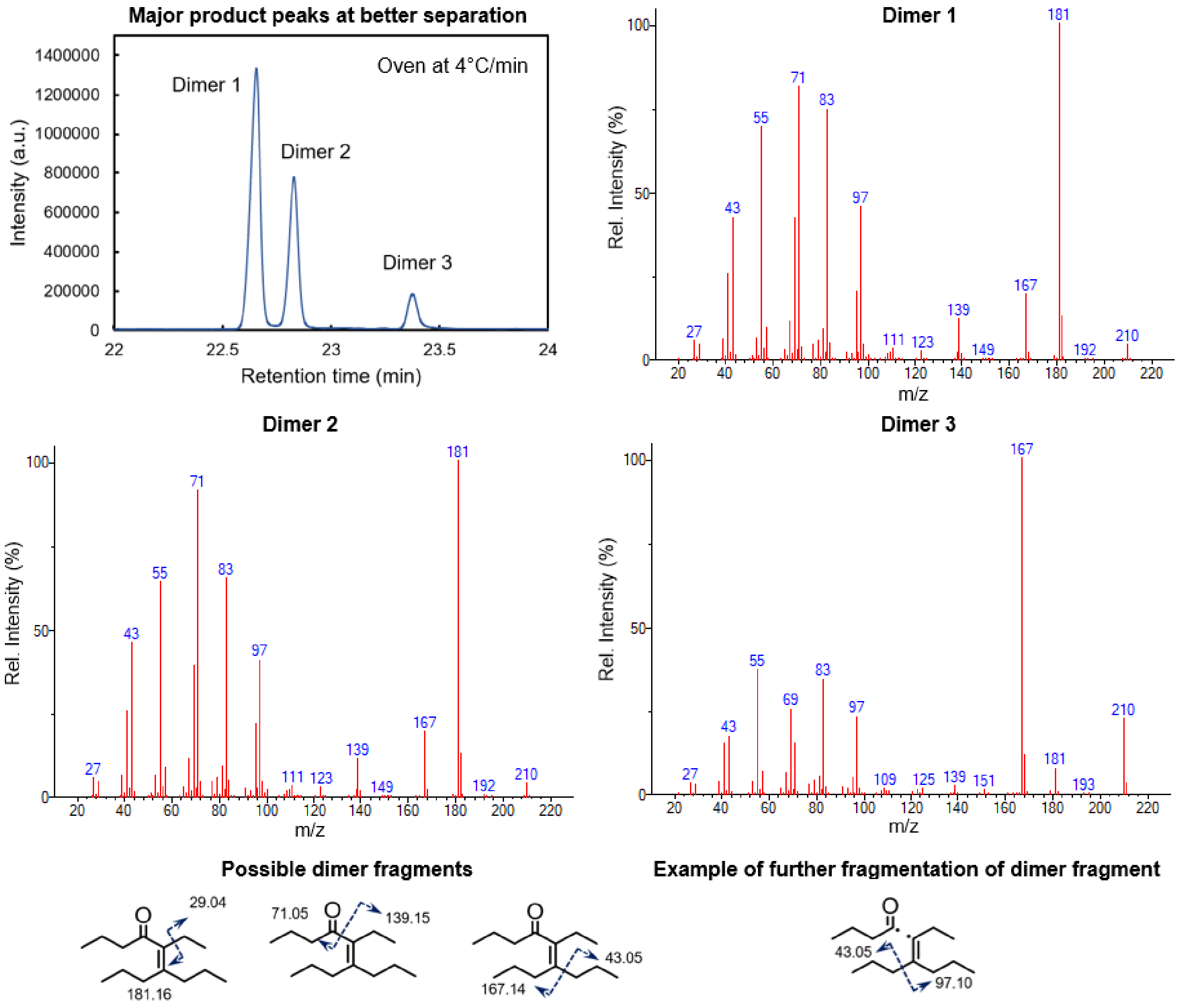

Major product peaks at better separation

Dimer 1

Dimer 2

Dimer 3

Possible dimer fragments

Example of further fragmentation of dimer fragment

Figure S4 GC-Polyarc/FID chromatogram and mass spectra of purified major product peaks at better separation by using lower oven temperature ramping rate. The major products were purified by spinning band distillation and used as standards for dimer quantification. The FID peak purity of the three major product peaks is >95%. A library search of their mass spectra in NIST database yielded low probability match due to the lack of dimer structure in the database, but the parent ion (210) and major product ions in the mass spectra are accessible from dimer fragmentation, supporting the major peaks being the target dimer.

Table S3 Carbon content, surface area and total acidity of fresh Nb_2O_5 and regenerated Nb_2O_5 in **Figure 2**.

Catalyst	**C content (wt.%)**	**Surface area (m^2 g^{-1})**	**Total acid sites (μmol g^{-1})**
Fresh Nb_2O_5	0	137	255
Regenerated Nb_2O_5 after 1 use	<0.1	123	266
Regenerated Nb_2O_5 after 4 uses	0.3	120	247

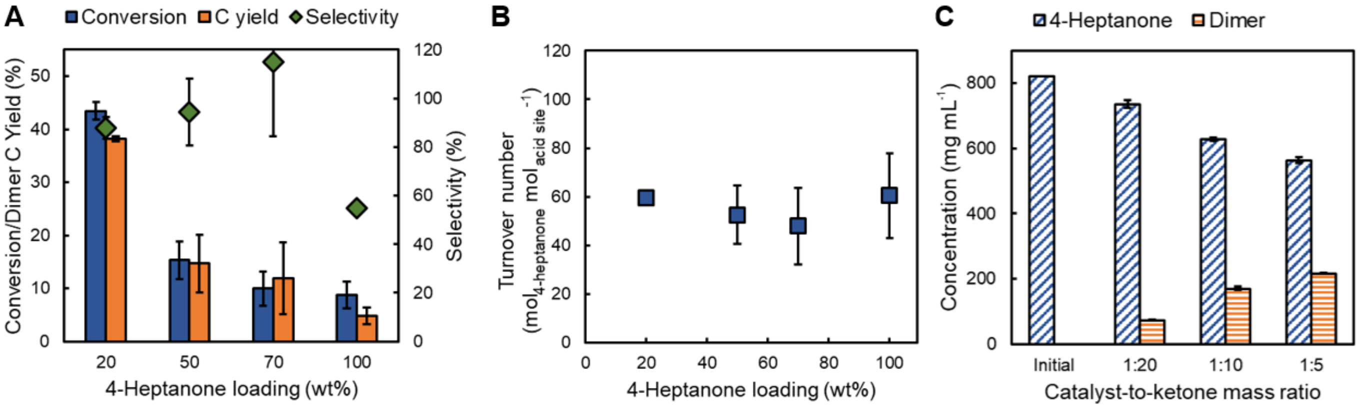

Figure S5 (A) 4-Heptanone condensation at varying ketone loadings (15 g feed, 0.75 g fresh Nb_2O_5, 20–100 wt.% 4-heptanone in toluene, corresponding catalyst-to-ketone mass ratio from 1:4 to 1:20, 180°C, 10 h). (B) Turnover number for 4-heptanone condensation (same reaction as figure A). (C) 4-Heptanone and dimer concentrations in the organic phase product at varying fresh Nb_2O_5 loadings (15 g feed, neat 4-heptanone, catalyst-to-ketone mass ratio from 1:20 to 1:5, 180°C, 24 h). All experiments were conducted in an initial He headspace at atmospheric pressure, stirring 800 rpm.

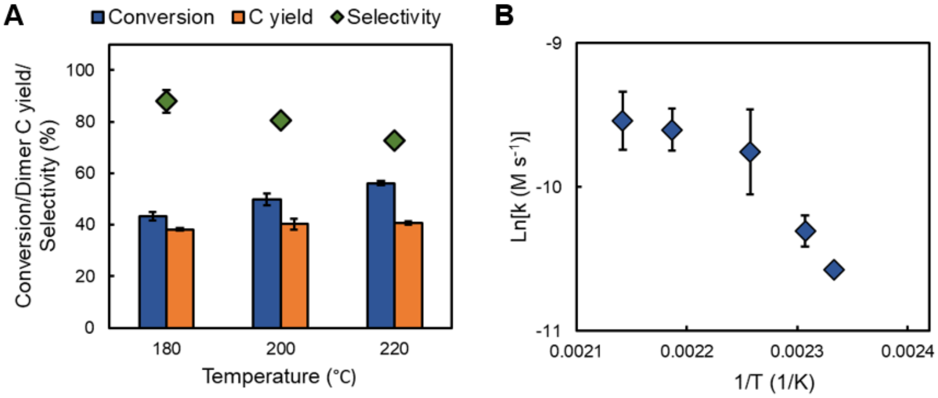

Figure S6 (A) Conversion of 4-heptanone at varying temperatures (15 g feed, 20 wt.% 4-heptanone in toluene, 0.75 g fresh Nb_2O_5, catalyst-to-ketone mass ratio = 1:4, 10 h). (B) Arrhenius plot for 4-heptanone condensation using initial rates at low conversion (8-22% for all tests). All experiments were conducted in an initial He headspace at atmospheric pressure, stirring 800 rpm.

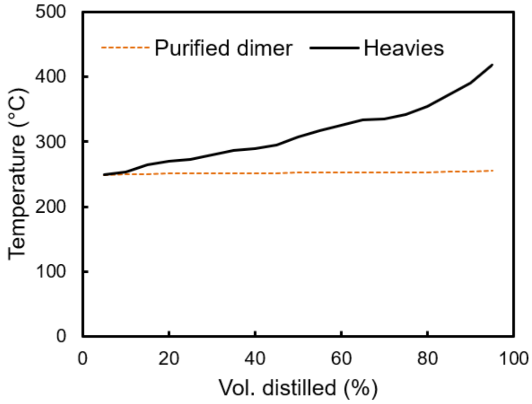

Figure S7 Simulated distillation curves of purified dimer and heavier compounds (heavies were obtained from removing dimer by distillation).

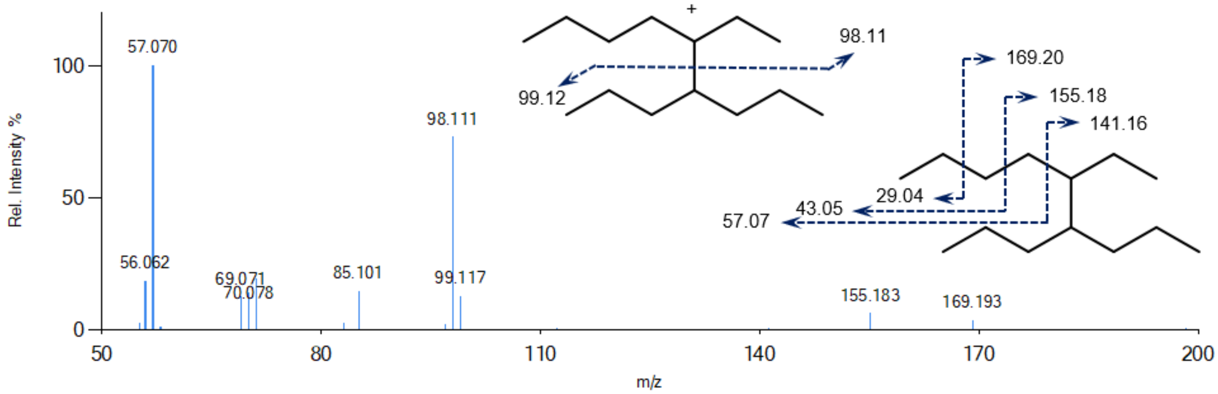

Figure S8 High resolution mass spectra of the C_{14} hydrocarbon.

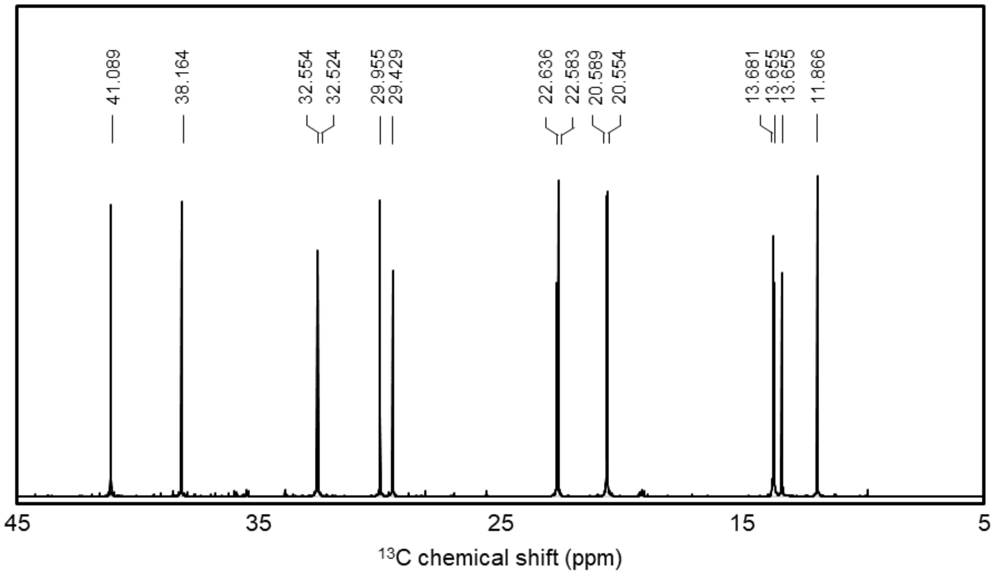

Figure S9 ^{13}C NMR spectrum of purified C_{14} hydrocarbon.

Table S4 Physicochemical properties of fresh and regenerated Pt/Al_2O_3.

Catalyst	**Pt content (wt.%)**	**Metal dispersion**	**Surface area (m^2 g^{-1})**	**Total acid sites (μmol g^{-1})**
Fresh	3.34	9.4%	198	1054
Regenerated	3.36	9.3%	197	1044

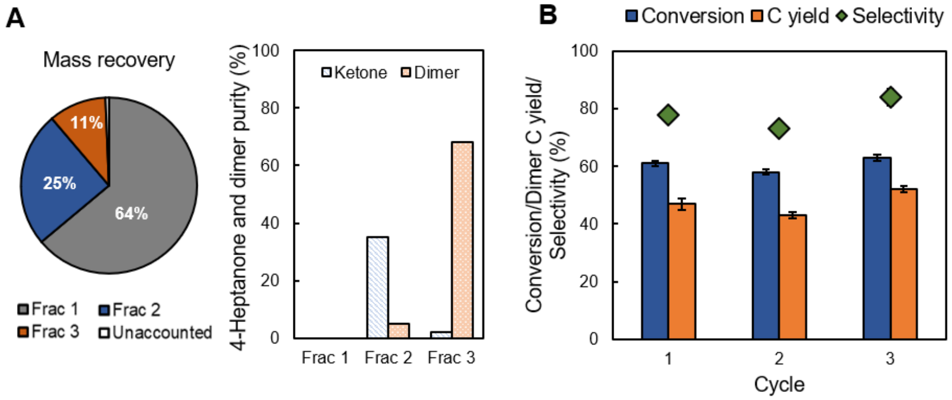

Figure S10 (A) Typical mass recovery and purities of 4-heptanone and target dimer product in three distillation fractions when distilling condensation product. (B) Conversion performance of recycled 4-heptanone using 20 wt.% commercial 4-heptanone as feed in the 1st cycle. Solvent and unreacted ketone were recovered by distillation, and additional 4-heptanone was added to match the initial 20 wt.% 4-heptanone loading before condensation testing of the recycled stream. Reaction conditions: 15 g feed, 0.75 g fresh Nb_2O_5, initial headspace at atmospheric pressure, 180°C, 24 h, stirring 800 rpm.

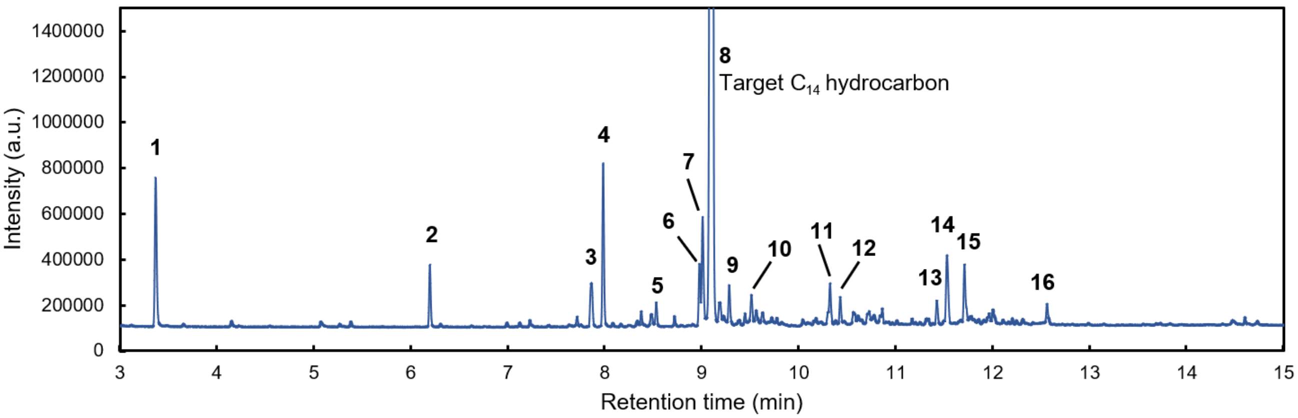

Peak #	Retention Time	Compound[a]	Potential C number	Prob%
1	3.369	heptane	C7	68.5
2	6.196	Heptane, 4-propyl-	C10	63.9
3	7.865	Octane, 2,3-dimethyl-	C10	38.0
4	7.983	Nonane, 5-butyl-	C13	27.7
5	8.531	Undecane, 5,6-dimethyl-	C13	15.2
6	8.977	Octane, 4,5-dipropyl-	C14	29.6
7	9.009	Tridecane, 4-methyl-	C14	9.34
8	9.106	Octane, 4,5-dipropyl-	C14	37.1
9	9.284	Cyclopropane, 1-(1,2-dimethylpropyl)-1-methyl-2-nonyl-	C18	12.4
10	9.513	6-Tridecene, 7-methyl-	C14	8.1
11	10.323	Benzene, 1,3-bis(1-methylpropyl)-	C14	33.1
12	10.428	Decane, 6-ethyl-2-methyl-	C13	9.1
13	11.425	Cyclohexane, 1,2,4,5-tetraethyl-, (1α,2α,4α,5α)-	C14	9.6
14	11.529	Dodecane, 2-methyl-8-propyl-	C16	8.6
15	11.709	Cyclohexane, 1,2,4,5-tetraethyl-, (1α,2α,4α,5α)-	C14	26.8
16	12.561	Benzene, 1,3,5-tri-tert-butyl-	C18	7.6

[a] Compound of highest probability identified in NIST database

Figure S11 GC-Polyarc/FID chromatogram and a list of relatively high intensity peaks for crude C_{14} blendstock from upgrading commercial butyric acid. Scale was adjusted to highlight minor components. Note that heavier condensation oligomers may not show on the chromatogram.

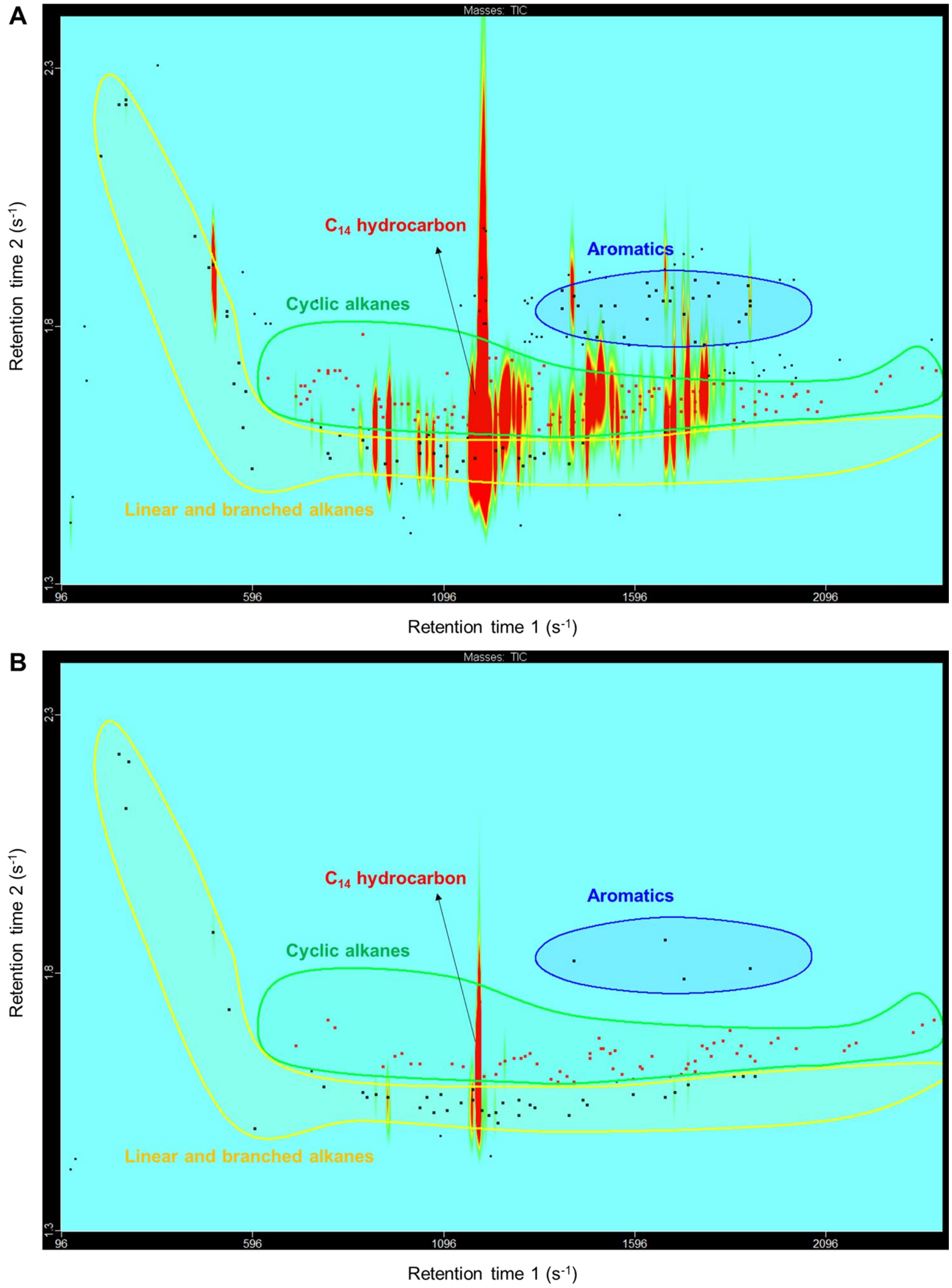

Figure S12 GC×GC-TOFMS chromatogram of crude hydrocarbon blendstock from upgrading commercial butyric acid: (a) dilution 20:1 and (b) dilution 400:1. The major component is the target non-cyclic C_{14} hydrocarbon. The most abundant classes present in the mixture are non-cyclic alkanes and cyclic alkanes, although there is potential overlap between these classes and ambiguous identification of linear alkanes and alkenes in these regions. Other structures identified in the plot include aromatics. Note that results are not quantitative.

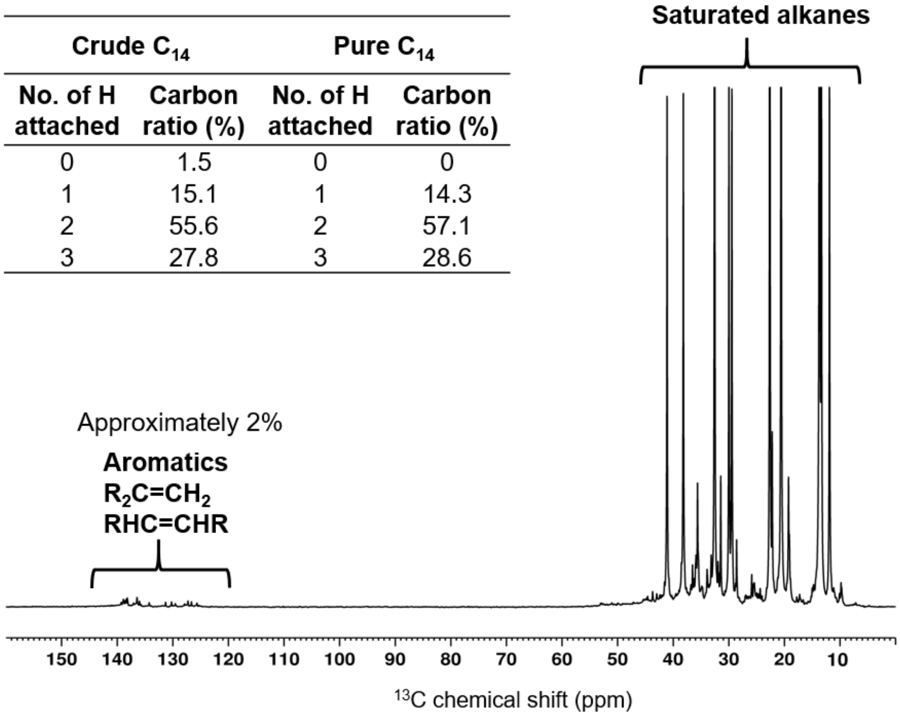

Crude C_{14}		Pure C_{14}	
No. of H attached	Carbon ratio (%)	No. of H attached	Carbon ratio (%)
0	1.5	0	0
1	15.1	1	14.3
2	55.6	2	57.1
3	27.8	3	28.6

Figure S13 ^{13}C NMR analysis of crude hydrocarbon blendstock from upgrading commercial butyric acid. The crude blendstock exhibited approximately 2% carbon in double bond or aromatic bond. Compared with pure C_{14} hydrocarbon, the crude blendstock displayed 3% decrease in the ratio of primary carbon. The ratio of carbon having two hydrogen attached (mostly secondary carbon) also decreased 3%. Accordingly, the ratio of carbon having one or no hydrogen attached (e.g., tertiary carbon, quaternary carbon, aromatic carbon) slightly increased.

Table S5 Concentrations of monomeric and total sugars in concentrated deacetylated dilute acid enzyme hydrolysate. Total sugars account for soluble oligomeric sugars.

concentration (g L^{-1})	**Sucrose**	**Glucose**	**Xylose**	**Galactose**	**Arabinose**	**Fructose**
Monomeric sugar	29.15	253.52	136.47	8.09	20.29	5.62
Total sugar	ND	292.80	149.29	8.46	19.96	1.35

ND = Not determined.

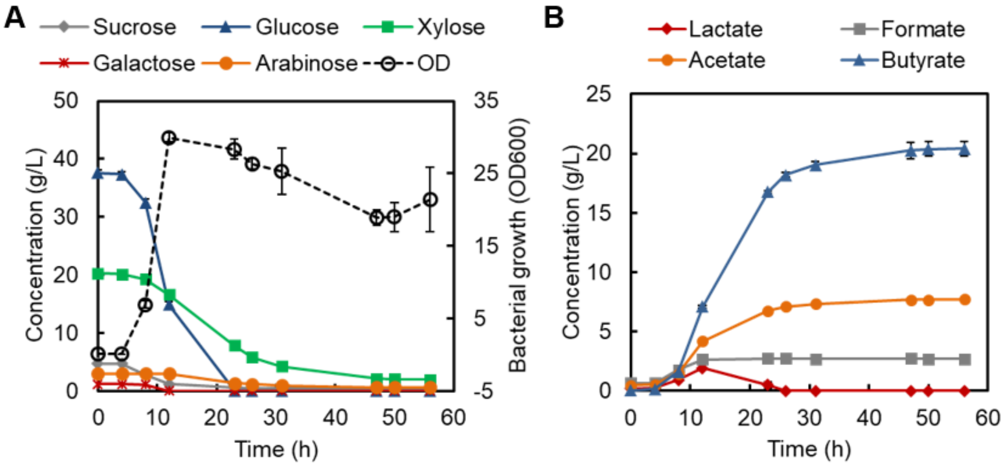

Figure S14 Batch conversion of lignocellulosic sugars by *Clostridium butyricum* (ATCC 19398). (A) Sugar utilization and bacterial growth measured as optical density at 600 nm (OD). (B) Butyric acid and byproducts formation. Data show the average of two biological replicates. Error bars represent the absolute difference between those replicates.

Table S6 Impurities in the acid feed and organic phase products from upgrading of biologically derived butyric acid

Element concentration (μg g^{-1})[a]	N[b]	S	Si	Ca	Na	P	K	B	Al	Fe	Ti	Mg
Bio-butyric acid feed	<2	<5	<100	<5	24	<1	<20	<5	<1	1	<0.1	<1
Ketonization product	<2	<5	160	<5	<10	<1	<20	<5	<1	<1	<0.1	<1
Condensation product	<2	<5	340	<5	<10	<1	<20	<5	1	<1	<0.1	<1
HDO product[c]	<2	<5	<100	<5	<10	<1	<20	<5	<1	<1	<0.1	<1

[a] Data obtained with ICP-AES.
[b] Data obtained with chemiluminescence, unit is mg L^{-1}.
[c] Before removing cyclohexane solvent.

Table S7 Additional fuel properties of clay-treated base diesel from Fioroni (2019)[12]

Property	Measurement	ASTM Method
Water and Sediment (°C)	<0.005	D2709
Water (μg/g)	37	D6304
Ash (mass %)	<0.001	D482
Sulfur (μg/g)	6.2	D5453
Copper Strip Corrosion	1A	D130
Aromatics (vol %)	31.6	D1319
Carbon Residue (mass %)	0.08	D524
Lubricity (μm)	520	D6079
Conductivity (pS/m)	1	D4308
Oxidation Stability (min)	68	D7545
Total Acid Number (mg KOH/g)	0.08	D664
Peroxide Value (mg/kg)	1	AOCS Cd 8b-90

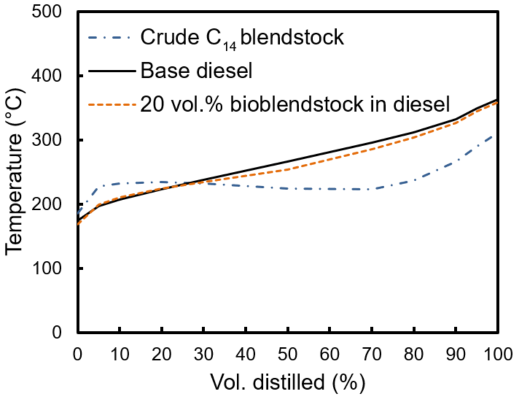

Figure S15 Simulated distillation curves of commercial butyric acid derived crude C_{14} blendstock, base diesel, and diesel blend with 20 vol.% bioblendstock (D86 correlation was applied to all three curves).

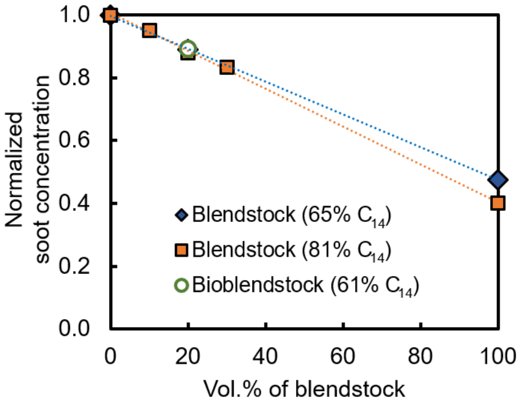

Figure S16 Plot of normalized soot concentration (NSC) over blend ratio of C_{14} blendstocks. Dotted lines are to guide the eye.

References

1. R. Nelson, D. Peterson, E. Karp, G. Beckham and D. Salvachúa, *Fermentation*, 2017, **3**, 10.
2. http://www.cambridgesoft.com/support/DesktopSupport/Documentation/Manuals/files/chemdraw_9_english.pdf.
3. *Estimation Programs Interface Suite™ for Microsoft® Windows, v 4.11*, United States Environmental Protection Agency, Washington, DC, USA, 2018.
4. M. Satou, S. Yokoyama and Y. Sanada, *Fuel*, 1992, **71**, 565-574.
5. R. W. Prugh, *Journal of Chemical Education*, 1973, **50**, A85.
6. R. M. Butler, G. M. Cooke, G. G. Lukk and B. G. Jameson, *Industrial & Engineering Chemistry*, 1956, **48**, 808-812.
7. W. G. Lloyd and D. A. Davenport, *Journal of Chemical Education*, 1980, **57**, 56.
8. R. Mott and C. Spooner, *Fuel*, 1940, **19**, 242.
9. W. Boie, *Energietechnik*, 1953, **3**, 309-316.
10. T. Kessler, E. R. Sacia, A. T. Bell and J. H. Mack, *Fuel*, 2017, **206**, 171-179.
11. D. D. Das, P. C. St. John, C. S. McEnally, S. Kim and L. D. Pfefferle, *Combustion and Flame*, 2018, **190**, 349-364.
12. G. Fioroni, L. Fouts, J. Luecke, D. Vardon, N. Huq, E. Christensen, X. Huo, T. Alleman, R. McCormick, M. Kass, E. Polikarpov, G. Kukkadapu and R. A. Whitesides, SAE Technical Paper 2019-01-0570, 2019.